Applied Catalysis B: Environmental 100 (2010) 338–345

Contents lists available at ScienceDirect

Applied Catalysis B: Environmental

journal homepage: www.elsevier.com/locate/apcatb

Preparation and characterization of magnetic TiO_2 nanoparticles and their utilization for the degradation of emerging pollutants in water

Pedro M. Álvarez[a,*], Josefa Jaramillo[a], Francisco López-Piñero[a], Pawel K. Plucinski[b]

[a] Departamento de Ingeniería Química y Química Física, Universidad de Extremadura, Avenida de Elvas S/N, 06071 Badajoz, Spain
[b] Department of Chemical Engineering, University of Bath, BA2 7AY Bath, United Kingdom

ARTICLE INFO

Article history:
Received 10 June 2010
Received in revised form 28 July 2010
Accepted 5 August 2010
Available online 12 August 2010

Keywords:
Emerging pollutants
Magnetic nanoparticles
Photocatalysis
Water treatment

ABSTRACT

Magnetic TiO_2/Fe_3O_4 and $TiO_2/SiO_2/Fe_3O_4$ nanoparticles (NPs) were prepared by an ultrasonic-assisted sol–gel method using a commercial nanosized magnetic iron oxide as a support. Magnetic NPs were characterized by X-ray diffraction (XRD), transmission electron microscopy (TEM), nitrogen adsorption (BET surface area) and SQUID magnetometer. Structure analyses indicated that TiO_2/Fe_3O_4 NPs presented a core–shell structure with a TiO_2 (anatase) coating wrapped around the magnetic iron oxide surface. $TiO_2/SiO_2/Fe_3O_4$ NPs showed a ternary structure with a core of Fe_3O_4, a SiO_2 mesosphere and a TiO_2 (anatase) crust. Both types of NPs exhibited magnetic properties with saturation magnetization about 40 emu/g and low remanent magnetization and coercivity. Stability of $TiO_2/SiO_2/Fe_3O_4$ NPs in an aqueous solution under UV illumination was better than that of TiO_2/Fe_3O_4 NPs as the presence of the insulation SiO_2 layer prevented photodissolution of iron. Both catalysts showed the ability to catalyze the photodegradation of acetaminophen and other four pharmaceutical and personal care products (PPCPs) (antipyrine, caffeine, metoprolol and bisphenol A) from an aqueous solution. In terms of catalytic activity the synthesized magnetic NPs were almost comparable to the commercial Degussa P25 TiO_2 photocatalyst. In addition, the easily recoverable magnetic photocatalysts showed good reusability, especially in the case of $TiO_2/SiO_2/Fe_3O_4$ NPs.

1. Introduction

TiO_2 photocatalysis is a well-known technology for removing organic and inorganic pollutants from water [1]. Because of its large band gap (around 3.2 eV), UV radiation ($\lambda < 385$ nm) can generate electron–hole pairs (e^-/h^+) that induce a series of reactions generating free-radicals which are very efficient oxidizers of adsorbed pollutants [2]. TiO_2 photocatalysis has recently attracted great interest as an efficient method for degrading refractory water pollutants using solar radiation as a light source [3]. Research studies have demonstrated that effective processing can be achieved by simply using Degussa P25 TiO_2 (composition: anatase and rutile 80:20; average particle size: 20–30 nm) in slurry-type photochemical reactors. This catalyst shows high photocatalytic activity in addition to good stability and relatively low cost [3,4]. However, a serious drawback of the process is the difficulty in separating the catalyst from the treated water at the exit of the photocatalytic reactor. A common way to perform the separation is by sedimentation of TiO_2 particles after pH adjustment and a coagulation–flocculation process. However, with this method a fraction of TiO_2 particles usually remains in the treated water and a further microfiltration step is usually required for final purification [5,6]. Separation by sedimentation can be enhanced by attaching TiO_2 particles onto other support particles like quartz, silica gel, alumina, zeolites, activated carbon or glass spheres but the loss of photocatalytic activity has usually been observed [7]. In this work a different approach to enhance the separation of TiO_2 is considered through the preparation of nanoparticles (NPs) with a magnetic core (Fe_3O_4) and a TiO_2 shell, so that they could be easily separated from the treated water under the application of an external magnetic field.

Synthesis and characterization of magnetic separable photocatalysts is an emerging area of concurrent research, being Beydoun and co-workers pioneer in this field [8–12]. Most of the magnetic photocatalysts developed so far contain a core of magnetite (Fe_3O_4), maghemite (γ-Fe_2O_3) or ferrite (e.g., $NiFe_2O_4$) and a shell of TiO_2. An intermediate layer barrier of SiO_2 between the magnetic core and the TiO_2 shell has been proposed to avoid photodissolution of iron and to prevent the magnetic core from acting as an electron–hole recombination centre, which would negatively affect the photoactivity of the catalyst [11–14]. TiO_2 magnetic photocatalysis has already been tested for the photodegradation of water pollutants, phenol and dyes in most of the cases (e.g., [15–18]).

* Corresponding author. Tel.: +34 924289385; fax: +34 924289385.
E-mail address: pmalvare@unex.es (P.M. Álvarez).

0926-3373/$ – see front matter © 2010 Elsevier B.V. All rights reserved.
doi:10.1016/j.apcatb.2010.08.010

Generally speaking, promising results were found in terms of photocatalytic activity, separability and catalyst stability.

In recent years, there is a great concern about the presence of pharmaceutical and personal care products (PPCPs) in water and wastewater, as they, even at small concentrations, might produce chronic toxicity, endocrine disruption and development of pathogen resistance. Since many of these substances escape to conventional wastewater treatments, they reach surface waters and distribute in the environment [19]. Therefore, there is an urgent need for the research and development of efficient treatment methods to completely remove these compounds, thus providing safe treated effluents. Photocatalysis with TiO_2 has been investigated with promising results for the degradation of a number of PPCPs (e.g., [20]). This paper reports on the synthesis of magnetic TiO_2/Fe_3O_4 and $TiO_2/SiO_2/Fe_3O_4$ nanoparticles (NPs) by a simple ultrasonic-assisted sol–gel method and their use for the photocatalytic removal and mineralization (i.e., TOC removal) of five selected PPCPs from aqueous solution.

2. Materials and methods

2.1. Materials

Magnetite (Fe_3O_4) NPs were kindly provided by Bendix S.A. (Spain) and used without further treatment. Titanium isopropoxide (TISOP), ethanolic tetraethyl orthosilicate (TEOS), isopropanol and aqueous NH_4OH solution (25% by volume) were obtained from Sigma–Aldrich. Powdered P25 TiO_2 was directly obtained from the manufacturer, Degussa AG (Germany). All five PPCPs (acetaminophen (Ac), antipyrine (Ant), caffeine (Caff), metoprolol (Met) and bisphenol A (BPA)) were supplied by Sigma–Aldrich (Spain) as pure compounds (>99%) and used without further purification.

2.2. Preparation of magnetic photocatalysts

After some preliminary research, the following method was adopted for direct TiO_2 surface coating of nanosized magnetic iron oxide (i.e., TiO_2/Fe_3O_4 NPs). First, 120 mg of Fe_3O_4 NPs were dispersed in 50 mL of isopropanol and sonicated for 15 min in an ultrasonic bath (Selecta JP Ultrasons). Then the dispersion was transferred to an Erlenmeyer flask where 50 mL of ultrapure water (Milli-Q, Millipore System) and 150 mL of isopropanol were added and the mixture was sonicated for 30 min. Next, a given amount of TISOP was added and the final reaction mixture was sonicated for 3 h. Temperature was controlled below 35 °C during sonication steps. The resulting catalytic particles were separated magnetically, washed three times with ethanol and dried overnight in an oven at 60 °C. The coated magnetic NPs were calcined at 400 °C for 1 h under static air.

To prepare $TiO_2/SiO_2/Fe_3O_4$ NPs, Fe_3O_4 NPs were first coated with SiO_2 and the resulting NPs were used as seed for the TiO_2 coating as described above. For the SiO_2 coating, 120 mg of nanosized Fe_3O_4 NPs were dispersed in 50 mL of isopropanol and sonicated for 15 min. Then, a mixture of 50 mL of water, 150 mL of isopropanol and 6 mL of NH_4OH were added and the mixture sonicated for 30 min, before adding 120 μL of TEOS. Hydrolysis of TEOS under alkaline conditions was carried out in an ultrasonic bath for 3 h. The coated particles were separated using an external permanent magnet, washed three times with ethanol and dried overnight in an oven at 60 °C.

2.3. Characterization of photocatalysts

X-ray diffraction patterns of the NPs were collected on a Philips PW1700 diffractometer with CuKα radiation (λ = 0.154 nm). TEM images were obtained with a JEOL JEM-2010 transmission electron microscope at an accelerating voltage of 200 kV. BET surface areas of the samples were obtained from nitrogen adsorption isotherms acquired with an Autosorb 1, Quantachrome apparatus and magnetic measurements were carried out at 300 K temperature using a Quantum Design MPMS XL SQUID magnetometer.

2.4. Photocatalytic experiments

Photodissolution and photodegradation experiments were carried out in bath mode at 25 °C using a jacketed photocatalytic reactor constructed with a central quartz well to introduce a low-pressure mercury lamp that emitted 254 nm radiation (Heraeus, model TNN 15/32). The intensity of the lamp was determined to be 3.8×10^{-6} einstein L^{-1} s^{-1} by carrying out experiments of photolysis of hydrogen peroxide (actinometer) as described elsewhere [21]. Agitation was provided by the bubbling of gas and by recirculating the liquid from the bottom to the top of the reactor at a flow rate of 10 L/h using a Masterflex (Cole Parmer) peristaltic pump.

For photodissolution experiments the photoreactor was loaded with 400 mL of phosphate-buffered ultrapure water and next a given mass of the catalyst was added once isothermal isothermal conditions (T = 298 K) were reached. At given interval, samples were withdrawn from the reactor. The magnetic NPs were separated using a permanent magnet (magnetic decantation) and the supernatant was analyzed for titanium and iron by means of atomic absorption spectroscopy using a Varian SpectrAA Series 140 apparatus. Control dissolution experiments were also carried out under the same conditions but with the UV lamp switched off.

Photodegradation experiments were carried out in the same experimental set-up and conditions described above. A pH 7 phosphate-buffered solution of either acetaminophen or a mixture of five PPCPs (Ac, Ant, Caff, Met and BPA) was photodegraded at 298 K for 5 h. Air was continuously supplied to the system at a flowrate of 50 L/h to keep the concentration of dissolved oxygen near its saturation. The aliquots were sampled from the reactor and filtered through a 0.2 μm PTFE filter to remove the photocatalyst particles, prior the analysis. The concentrations of target compounds in samples were measured by HPLC using a HP1110 Series chromatograph connected to a UV detector. For the analysis of acetaminophen a 1 mL/min flowrate of mixture of acetonitrile and water (15:85 v/v) acidified with phosphoric acid (0.1%) as a mobile phase and a Trazer Kromasil-100 (C18; 15 cm × 0.4 cm, 5 μm) column were used. The detection was set at 244 nm. The same procedure was used for the multicomponent analysis of the PPCPs mixture but the mobile phase flowrate was set at 0.65 mL/min and detection was made at different wavelengths (225 nm, 240 nm, 244 nm, 273 nm and 280 nm for metoprolol, antipyrine, acetaminophen caffeine and bisphenol A, respectively). Total organic carbon (TOC) was also analyzed with a Shimadzu TOC-V_{CSH} apparatus.

3. Results and discussion

3.1. Characterization of magnetic photocatalysts

Table 1 summarizes the composition and other relevant properties of the magnetic iron oxide used as seed and photocatalysts prepared in this investigation.

All solids presented type IV adsorption isotherms (not shown), characteristic of non-porous materials. BET surface area of nano-

Table 1
Some properties of the NPs used in this work.

NP sample	Composition (wt.%)	Crystallite sizes (nm)	S_{BET} (m^2/g)	M_S (emu/g)	M_R (emu/g)	H_c (Oe)
Magnetic iron oxide	Fe_3O_4 100%	M (25.8)	42	78.9	1.2	7.1
Degussa P25 TiO_2	TiO_2 100%	A (20.3)	47	–	–	–
TiO_2/Fe_3O_4	Fe_3O_4 57.1% TiO_2 42.9%	M (26.4) A (14.5)	27	44.3	3.6	48.2
$TiO_2/SiO_2/Fe_3O_4$	Fe_3O_4 49.3% SiO_2 14.3% TiO_2 37.4%	M (27.2) A (15.6)	22	39.3	2.9	53.0

sized magnetic iron oxide and Degussa P25 TiO_2 were found to be 42 and 47 m^2/g, respectively, which are close to the values given by the suppliers (49 and 53 m^2/g). TiO_2/Fe_3O_4 and $TiO_2/SiO_2/Fe_3O_4$ NPs presented lower surfaces areas than the magnetic iron oxide seed particles likely due to the increase of the overall particle size as a result of the coating process.

Fig. 1 shows the XRD patterns of TiO_2/Fe_3O_4 and $TiO_2/SiO_2/Fe_3O_4$ NPs before and after the calcination stage. The diffractograms of nanosized magnetic iron oxide and Degussa P25 TiO_2 are also shown. XRD patterns of the magnetic iron oxide used as seed match well with the standard patterns for bulk magnetite (JCPDS File no. 19-0629). Though the presence of maghemite as a result of partial oxidation of magnetite could not be ruled out from XRD results since magnetite and maghemite (JCPDS File no. 39-1346) show very similar XRD patters, precautions were taken to avoid oxidation so that it can be considered that the particles consisted mainly of Fe_3O_4. Although less intense, the peaks of magnetite can be observed in all other diffractograms of Fig. 1. The size of Fe_3O_4 crystallites was estimated using the Scherrer equation applied to the (3 1 1) plane of the spinel reflections. As shown in Table 1, a mean particle size of 25.8 nm was calculated for support Fe_3O_4 NPs and it remained practically unchanged after the sol–gel method. The diffractogram of Degussa P25 TiO_2 evidence the presence of anatase (JCPDS File no. 21-1272) and to a lesser extent rutile (JCPDS File no. 21-1276), as expected according to the composition given by the manufacturer (anatase 80%, rutile 20%). No peaks of anatase nor rutile can be distinguished in the diffactograms of TiO_2/Fe_3O_4 and $TiO_2/SiO_2/Fe_3O_4$ NPs before calcination. However, after the calcinations the anatase peaks appeared, indicating that upon calcination crystallites of anatase were mainly formed from the amorphous titanium dioxide deposited on the magnetite with the sol–gel method. The average crystallite sizes of TiO_2 deposited onto magnetic NPs, as calculated by applying the Scherrer equation to the anatase (1 0 1) peak, were lower than that of anatase crystallites on Degussa P25 particles. No peaks of SiO_2 (JCPDS File no. 20-1050) can be observed in the diffractogram of $TiO_2/SiO_2/Fe_3O_4$ NPs which reveals that amorphous SiO_2 formed a layer over the magnetic iron oxide. Another noticeable experimental evidence of XRD analysis is the absence of peaks characteristics of hematite (JCPDS File no 33-0664) in the magnetic photocatalysts. Also, no change of colour from brown to orange was observed in the NPs upon heat treatment. This means that at the calcination conditions applied no oxidation of the magnetic iron oxide core to hematite was produced.

Fig. 2 shows TEM images of TiO_2/Fe_3O_4 and $TiO_2/SiO_2/Fe_3O_4$ NPs. It can be seen that both kind of NPs show a roughly spherical morphology with aggregates of magnetic iron oxide particles surrounded by a matrix of TiO_2 or SiO_2 and TiO_2. These clusters are organized in chain structures likely due to the magnetic dipole interaction between neighbouring particles. It can be seen that in a TiO_2/Fe_3O_4 NPs a TiO_2 coating layer (bright shell) is wrapped about the surface of magnetic iron oxide particles (black core) forming a TiO_2/Fe_3O_4 core–shell structure while in $TiO_2/SiO_2/Fe_3O_4$ NPs a ternary structure with a core of Fe_3O_4 (black) a SiO_2 layer (bright) and a TiO_2 outer layer (bright) can be seen.

Magnetic properties of seed magnetic iron oxide, TiO_2/Fe_3O_4 and $TiO_2/SiO_2/Fe_3O_4$ NPs were measured at 300 K as illustrated in Fig. 3. The values of saturation magnetization (M_S), remanent

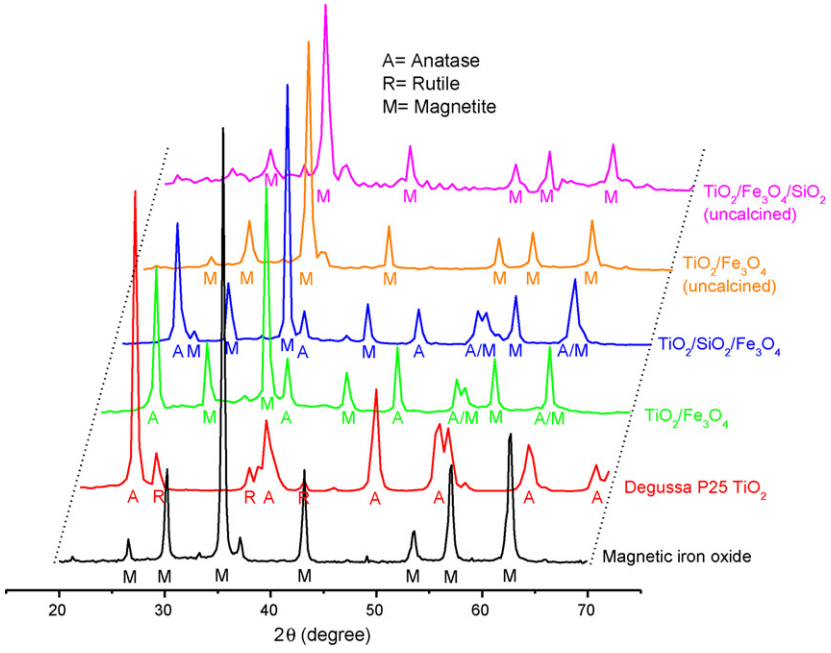

Fig. 1. XRD patterns of various NPs.

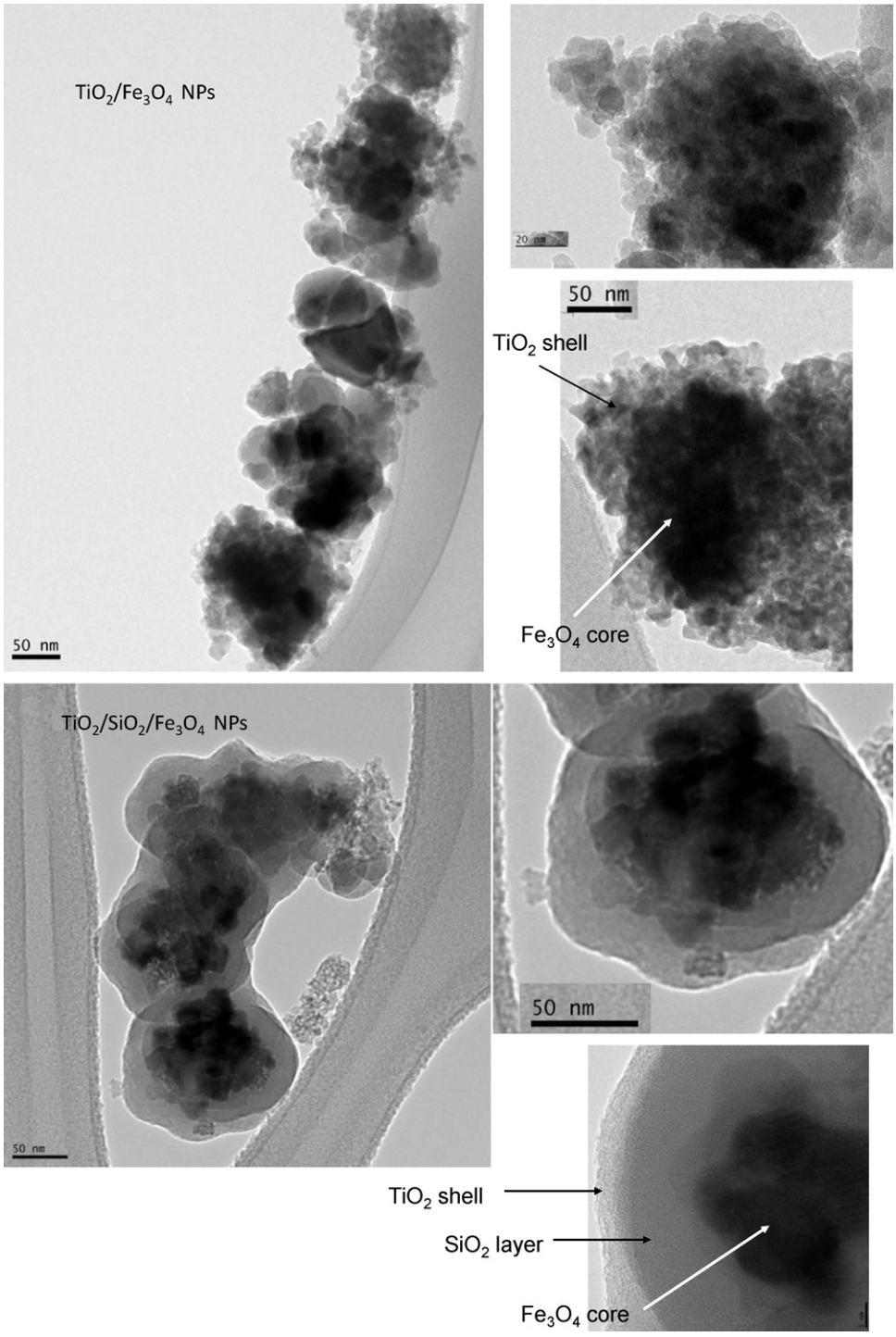

Fig. 2. TEM images of TiO_2/Fe_3O_4 and $TiO_2/SiO_2/Fe_3O_4$ NPs.

magnetization (M_r) and coercivity (H_C) are shown in Table 1. The observed value of saturation magnetization for the magnetic iron oxide particles used as seed was found to be lower than that of bulk magnetite (92 emu/g) but in the range of experimental values reported elsewhere (e.g., [16]). The decrease in the saturation magnetization with the coating processes is due to the lower content of magnetic iron oxide in the photocatalysts and the presence of non-magnetic coating layers (TiO_2 and SiO_2). Thus, considering the Fe_3O_4 percentages given in Table 1, maxima M_S values of 45.0 and 38.9 emu/g would be expected for TiO_2/Fe_3O_4 and $TiO_2/SiO_2/Fe_3O_4$ NPs. As can be seen in Table 1, the measured values were close to them, indicating that the coating does not change to a great extent the magnetic properties of the particles. The superparamagnetic behaviour of the synthesized NPs at room temperature can be inferred from their low values of remanence magnetization and coercivity. Accordingly, particles did not aggregate so much after being separated by a magnet.

3.2. Dissolution and photodissolution

Prior to photodegradation experiments a series of dissolution and photodissolution experiments were carried out to ascertain

Table 2
Leaching of iron from the NPs during dissolution and photodissolution experiments.

Photocatalyst	Absence of UV radiation			Presence of UV radiation		
	pH = 3	pH = 5	pH = 7	pH = 3	pH = 5	pH = 7
TiO_2/Fe_3O_4 NPs	0.22%	0.17%	0.09%	4.36%	3.44%	3.35%
$TiO_2/SiO_2/Fe_3O_4$ NPs	0.12%	0.10%	0.07%	0.15%	0.16%	0.09%

the stability of NPs under process conditions. The concentration of iron and titanium was measured after 2 h-batch experiments. While the titanium concentration was always found to be below the detection limit of the AAS apparatus, the concentration of the iron was as high as 12 mg/L in some experiments. Table 2 summarizes the percentage of leached iron determined from mass-balance calculations performed on the basis of the catalyst composition (see Table 1), the catalyst loading and the amount of iron found in the solution. From the results of Table 2 it can be observed that, in the absence of UV radiation, the two kinds of particles were rather stable in the aqueous solution even at acidic pH. In fact, the coating markedly improved the stability of Fe_3O_4 NPs as about 1.4% of iron was leached out from the magnetic iron oxide in a dissolution experiment at pH 3. In the presence of UV radiation (i.e., photodissolution experiments) the stability of TiO_2/Fe_3O_4 NPs markedly decreased while the stability of $TiO_2/SiO_2/Fe_3O_4$ NPs did not depend on the presence of the illumination source. These results qualitatively agree with those of Beydoun et al. [8–11] who attributed the poorer stability of TiO_2/Fe_3O_4 NPs to the effect of electrons generated from the photoactivation of TiO_2 that could be transferred to the conduction band of Fe_3O_4, thus producing iron ions that migrate to the solution. The presence of an insulating SiO_2 layer in $TiO_2/SiO_2/Fe_3O_4$ NPs prevents electrons from being transferred to the magnetic iron oxide core thus avoiding iron leaching.

3.3. Photocatalytic activity

3.3.1. Photodegradation of acetaminophen

Acetaminophen (Ac), a pharmaceutical of widespread use, was first chosen as a target compound to test the photocatalytic activity of the prepared photocatalysts. Fig. 4 shows the concentration profiles of Ac during photodegradation experiments in the presence of different NPs. From Fig. 4 it is apparent that Ac was partly photolyzed under UV illumination in the absence of a catalyst, as a consequence of its high molar extinction coefficient ($\varepsilon_{254\,nm} \approx 750\,M^{-1}\,s^{-1}$) [22]. The rate of Ac removal in the presence of 1 g/L of magnetic iron oxide NPs was even lower than in the absence of NPs, indicating that these NPs do not show catalytic activity towards Ac photodegradation. The lowering of Ac conversion in the presence of magnetite NPs can be due to less efficient direct photolysis of Ac because of light dispersion produced by the suspended NPs. The rate of Ac removal was greatly enhanced by the presence of Degussa P25 TiO_2, TiO_2/Fe_3O_4 or $TiO_2/SiO_2/Fe_3O_4$ NPs. Thus, in the presence of any of these catalysts almost complete conversion of Ac was achieved in 5 h while in the absence of a catalyst barely a 30% Ac conversion was attained. As titania is regarded as the only active species in the prepared NPs, for comparative purposes, we used similar TiO_2 loading (0.5 g TiO_2/L) in experiments with Degussa P25 TiO_2 and with the two types of TiO_2-based NPs prepared. From Fig. 4 it can be deduced that the photocatalytic activity shown by $TiO_2/SiO_2/Fe_3O_4$ NPs was close to that of Degussa P25 TiO_2, while TiO_2/Fe_3O_4 NPs were slightly less efficient towards Ac photodegradation. In terms of Ac mineralization, TOC removal after 5 h of photodegradation was 4.1% in the absence of a catalyst while it was found to be 43.5%, 30.8% and 39.7% in experiments carried out with Degussa P25 TiO_2, TiO_2/Fe_3O_4 and $TiO_2/SiO_2/Fe_3O_4$ NPs, respectively. These results indicate that TiO_2 photocatalysis was more efficient than direct photolysis not only in degrading the parent compound (Ac) but its reaction intermediates, which are reported to be N-(3,4-dihydroxypehnyl)-acetamide, N-(2,4-dihydroxyphenyl)-acetamide, hydroquinone, acetamide and several short-chain carboxylic acids [22].

The photolysis of TiO_2 in water generates electrons and positive holes (e^-/h^+) which, at oxic conditions, give rise to the formation of hydroxyl ($HO^\bullet$) and superoxide radicals ($^\bullet O_2^-$) that are the primary reactive species in the photocatalytic oxidation of water pollutants [2]. According to the literature [22,23], the hydroxyl radicals are responsible for major degradation of Ac by TiO_2 photocatalysis being the second-order rate constant of the reaction between $HO^\bullet$

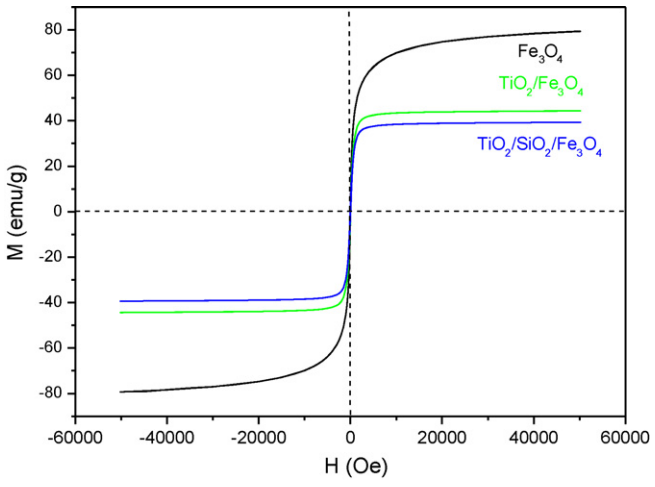

Fig. 3. Magnetic hysteresis loop at 300 K of magnetic iron oxide (Fe_3O_4), TiO_2/Fe_3O_4 and $TiO_2/SiO_2/Fe_3O_4$ NPs.

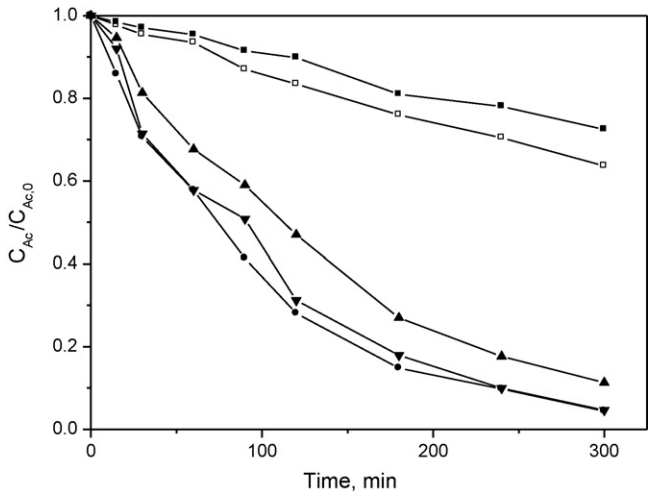

Fig. 4. Photodegradation of acetaminophen in aqueous solution in the absence (blank) and presence of different NPs. Reaction conditions: $T \sim 25\,^\circ C$; pH = 7; $C_{Ac,0}$ = 30 mg/L; catalyst and dose: (□) none (blank experiment); (■) magnetic iron oxide, 1.0 g/L; (●) Degussa P25 TiO_2, 0.5 g/L; (▲) TiO_2/Fe_3O_4, 1.16 g/L; (▼) $TiO_2/SiO_2/Fe_3O_4$ 1.34 g/L.

Table 3
Apparent first-order rate constant ($k_{app} \times 10^3$/min) for the photodegradation of acetaminophen and a mixture of five PPCPs at pH 7.

Photocatalyst	Single-solute solution	Equimolar mixture of five PPCPs				
	Ac	Ac	BPA	Met	Ant	Caff
None	1.49 ± 0.02	0.68 ± 0.03	0.52 ± 0.02	0.63 ± 0.03	0.82 ± 0.03	0.72 ± 0.02
Degussa P25 TiO_2	10.21 ± 0.14	7.96 ± 0.07	15.81 ± 0.24	13.81 ± 0.64	10.91 ± 0.21	10.51 ± 0.24
TiO_2/Fe_3O_4	7.11 ± 0.13	4.86 ± 0.07	11.68 ± 0.31	10.15 ± 0.28	8.65 ± 0.22	9.29 ± 0.20
$TiO_2/SiO_2/Fe_3O_4$	9.79 ± 0.21	7.44 ± 0.20	15.09 ± 0.24	13.21 ± 0.40	9.97 ± 0.16	10.89 ± 0.20

and Ac as high as 1.7×10^9 M^{-1} s^{-1}. The lower photocatalytic activity of TiO_2/Fe_3O_4 NPs observed in our experiments can be due to the direct contact between the iron oxide core and the TiO_2 shell [11]. Thus, a part of the electrons generated from the photolysis of TiO_2 would migrate to the Fe_3O_4 core and produce the diffusion of iron ions through the titania shell towards the liquid bulk (2.93% of iron was leached out from the magnetic core). In addition to the reduction in the number of electrons available to produce photooxidants, the Fe(II) ions, once in solution, would compete with Ac for oxidants, thereby decreasing the rate of Ac degradation. On the other hand, it should be considered that the presence of Fe(III) ions in solution can enhance the efficiency of TiO_2 photocatalysis as they can act as electron acceptors avoiding electron–hole recombinations [24]. However, it is reported that this synergy between Fe(III) and TiO_2 photocatalysis is only dominant at pH < 3.5. Beyond this pH, the activity decreases due to the precipitation of iron species [25].

The kinetics of TiO_2 photocatalytic degradation of organic compounds is usually modelled using a Langmuir–Hinshelwood approach. In accordance with this, Eq. (1) could be used to describe the rate of Ac degradation over TiO_2-based photocatalyst:

$$-r_{Ac} = -\frac{dC_{Ac}}{dt} = \frac{K_{Ac} \times k \times C_{Ac}}{1 + K_{Ac} \times C_{Ac}} \quad (1)$$

where K_{Ac} is the adsorption constant of Ac over the catalyst and k stands for the intrinsic rate constant. The results of adsorption experiments of Ac over Degussa P25 TiO_2, TiO_2/Fe_3O_4 and $TiO_2/SiO_2/Fe_3O_4$ NPs in the absence of UV source showed that Ac did not adsorb appreciably over these solids (less than 2% Ac removal from aqueous solution in 5-h batch experiments). Thus the weak adsorption of Ac on the catalysts' surfaces can be considered and therefore $K_{Ac} \times C_{Ac} \ll 1$. Accordingly, Eq. (1) can be simplified by an apparent first-order kinetics. Once integrated, Eq. (2) is obtained:

$$\ln \frac{C_{Ac}}{C_{Ac,0}} = K_{Ac} \times k \times t = -k_{app} \times t \quad (2)$$

From the regression analyses of experimental data according to Eq. (2), the values of k_{app} for the degradation of Ac at pH 7 by direct photolysis and photocatalysis using different NPs were obtained as summarized in Table 3 (all the regressions generated showed $r^2 > 0.98$). The results reflect a higher apparent rate constant for Degussa P25 TiO_2 but very close to that for $TiO_2/SiO_2/Fe_3O_4$. From that, one can see that the catalytic activity of synthesized $TiO_2/SiO_2/Fe_3O_4$ is almost the same as that of Degussa P25 TiO_2. Taking into account the possibility of simple recycling of magnetite-based catalyst in external magnetic field, the $TiO_2/SiO_2/Fe_3O_4$ photocatalyst can be considered as effective alternative for the Degussa P25 TiO_2 catalyst.

3.3.2. Photodegradation of a mixture of PPCPs

Fig. 5 shows the concentration profiles of acetaminophen (Ac), antipyrine (Ant), caffeine (Caff), metoprolol (Met) and bisphenol A (BPA) during the course of photodegradation experiments. It can be seen that in the absence of a catalyst, the degradation of any of the PPCPs was rather poor with less than 20% removal in a 5-h experiment. In contrast, in the presence of TiO_2 photocatalysts (either Degussa P25, $TiO_2/SiO_2/Fe_3O_4$ or TiO_2/Fe_3O_4) all the PPCPs except Ac were degraded by more than 95% within this treatment time. The application of Eq. (2) to the data presented in Fig. 5 enabled the determination of the apparent first-order rate constant for the photodegradation of each compound in the mixture. The calculated values are summarized in Table 3. As can be seen, Ac exhibited lower apparent photodegradation rate constant in the aqueous mixture than in the single-solute solution, suggesting competitive kinetics. The order of the calculated apparent rate constants (BPA > Met > Caff ≈ Ant > Ac) matches well with the order of the reported values of the rate constants between the hydroxyl radical and the selected compounds ($k_{HO\cdot-BPA} = 10.2 \times 10^9$ M^{-1} s^{-1} [26] > $k_{HO\cdot-Met} = 6.8 \times 10^9$ M^{-1} s^{-1} [27] > $k_{HO\cdot-Caff} = 5.9 \times 10^9$ M^{-1} s^{-1} [28] > $k_{HO\cdot-Ant} = 5.2 \times 10^9$ M^{-1} s^{-1} [29] > $k_{HO\cdot-Ac} = 1.7 \times 10^9$ M^{-1} s^{-1} [22]), which confirms that hydroxyl radical oxidation was the main route of the PPCPs' photodegradation. The TOC graph in Fig. 5 clearly shows that the TOC conversion was limited, with less than 60% PPCPs mineralization even when Degussa P25 TiO_2 was used as catalyst. Therefore more severe oxidation conditions (i.e., higher reaction time, UV lamp intensity and/or photocatalyst dose) would be needed to reach complete mineralization. All graphs in Fig. 5 show similar concentration profiles, indicating that the photocatalytic activity of $TiO_2/SiO_2/Fe_3O_4$ NPs was close to that of Degussa P25 TiO_2 and somewhat higher than that of TiO_2/Fe_3O_4 NPs for any of the PPCPs in the mixture. Regarding catalyst stability, the percentage of iron leached out from TiO_2/Fe_3O_4 and $TiO_2/SiO_2/Fe_3O_4$ NPs was found to be, as average, 2.37% and 0.11%, respectively, which demonstrated a much higher stability of the catalyst with the intermediate SiO_2 layer.

3.3.3. Photocatalyst reusability

Another important issue is whether the catalytic activity of magnetic TiO_2 NPs can be sustained throughout their repetitive use. To test the reusability of synthesized photocatalysts two parallel sets of Ac degradation experiments were carried out with TiO_2/Fe_3O_4 and $TiO_2/SiO_2/Fe_3O_4$ NPs. In both sets of experiments four 5-h batches were completed. After each batch the agitation was stopped and the NPs were allow to be separated by a permanent magnet for 1 h. Then, the aqueous solution was removed from the photoreactor and replaced by a fresh aqueous solution of Ac. Fig. 6 shows the results of the apparent first-order rate constant calculated by applying Eq. (2) to the data set for each batch. When $TiO_2/SiO_2/Fe_3O_4$ NPs were used only a slight decrease in the apparent rate constant with the number of uses was observed. Thus, after the four batches k_{app} decreased by less than 10%, demonstrating this catalyst to be reusable. On the other hand, the loss of catalytic activity was more pronounced for TiO_2/Fe_3O_4 NPs as k_{app} diminished by about 30% after the four batches. It is believed that the main reason for the observed catalytic activity losses is due to catalyst mass losses during the separation stage. The large difference between $TiO_2/SiO_2/Fe_3O_4$ and TiO_2/Fe_3O_4 NPs is most likely due to the leaching of iron from TiO_2/Fe_3O_4 and therefore the loss of ability to be separated magnetically of

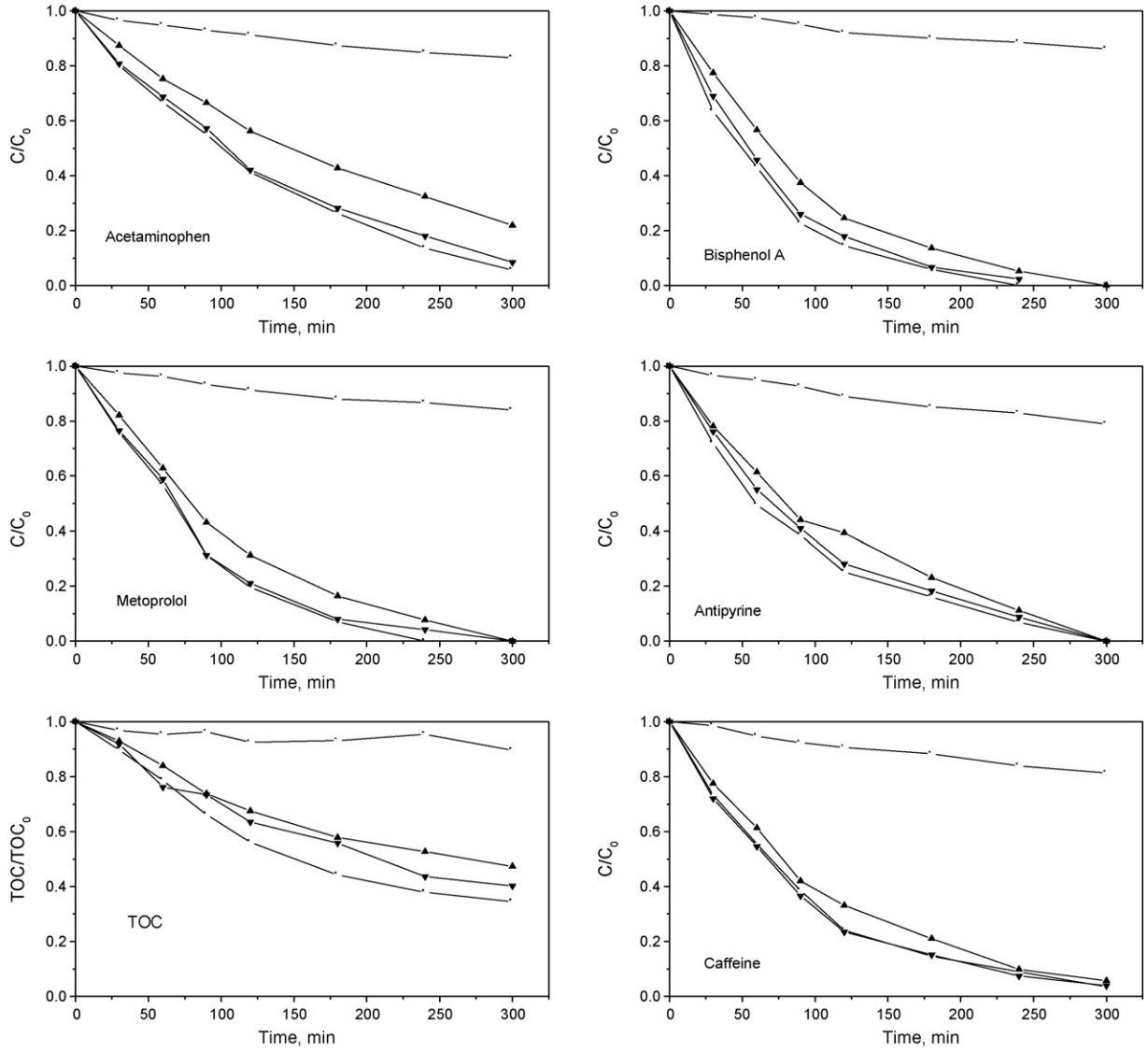

Fig. 5. Photodegradation of a mixture of five PPCPs in aqueous solution in the absence (blank) and presence of different NPs. Reaction conditions: $T \sim 25\,^{\circ}C$; pH = 7; $C_{Ac,0}$ = 30 mg/L; catalyst and dose: (□) none (blank experiment); (●) Degussa P25 TiO_2, 0.5 g/L; (▲) TiO_2/Fe_3O_4, 1.16 g/L; (▼) $TiO_2/SiO_2/Fe_3O4$, 1.34 g/L.

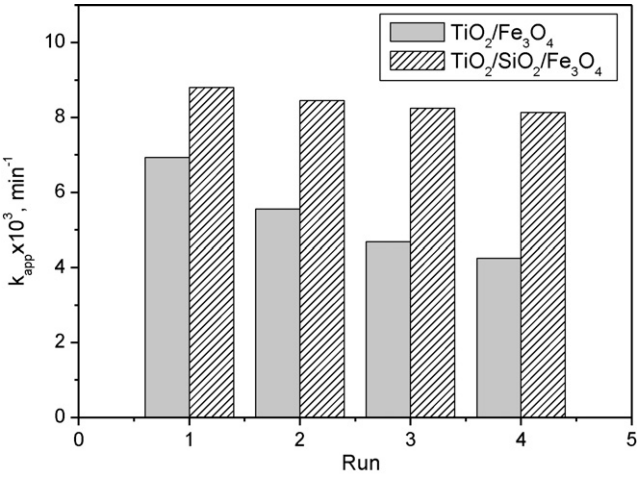

Fig. 6. Effect of photocatalyst reusability on the apparent first-order rate constant for the photodegradation of Ac in aqueous solution. Reaction conditions: $T \sim 25\,^{\circ}C$; pH = 7; $C_{Ac,0}$ = 30 mg/L; catalyst and dose: TiO_2/Fe_3O_4, 1.16 g/L; $TiO_2/SiO_2/Fe_3O_4$, 1.34 g/L.

TiO_2/Fe_3O_4 NPs as far as they are used in photodegradation experiments.

4. Conclusions

Although Degussa P25 TiO_2 remains the most widely used photocatalyst in water treatment, the difficulty in its separation because of its small size prompt to the search of alternative materials. In this work, we synthesized magnetic TiO_2/Fe_3O_4 or $TiO_2/SiO_2/Fe_3O_4$ NPs which were demonstrated to be easily separable by an external magnetic field. The application of the prepared NPs as a photocatalyst was evaluated by degrading acetaminophen and other four PPCPs from the aqueous solution. The $TiO_2/SiO_2/Fe_3O_4$ photocatalyst was almost as effective as Degussa P25 TiO_2 and showed good reusability as no loss of efficiency was observed within four repetitive experiments reusing the catalyst. Given the promising results of this study, new research is being carried out on the use of magnetic TiO_2 catalysts for the degradation of PPCPs in water and wastewater by UV–A radiation (λ = 365 nm) and solar detoxification methods.

Acknowledgements

This collaborative work has been financed by the Junta de Extremadura and FEDER Funds projects Ref. PDT08-A12 and GRU09009 (Spain) and EPSRC Research Grant No. EP/D064937/1 (UK). Dr J. Jaramillo also thanks the Consejería de Educación of Junta de Extremadura for providing her with a sabbatical research year.

References

[1] A.L. Linsebigler, L. Guanquan, J.T. Yates, Chem. Rev. 95 (1995) 735–758.
[2] J.M. Herrmann, Top. Catal. 34 (2005) 49–65.
[3] S. Malato, P. Fernández-Ibañez, M.I. Maldonado, J. Blanco, W. Gernjak, Catal. Today 141 (2009) 1–59.
[4] J. Blanco-Gálvez, P. Fernández-Ibañez, S. Malato-Rodríguez, J. Sol. Energy Eng. 129 (2007) 4–15.
[5] R.J. Watts, S. Kong, W. Lee, J. Environ. Eng. 121 (1995) 730–735.
[6] P. Fernández-Ibañez, J. Blanco, S. Malato, F.J. de las Nieves, Water Res. 37 (2003) 3180–3188.
[7] V. Loddo, G. Marcí, L. Palmesano, A. Sclafani, Mater. Chem. Phys. 53 (1998) 217–224.
[8] D. Beydoun, R. Amal, G.K.C. Low, S. McEvoy, J. Phys. Chem. B 104 (2000) 4387–4396.
[9] D. Beydoun, R. Amal, J. Scott, G. Low, S. McEvoy, Chem. Eng. Technol. 24 (2001) 745–748.
[10] D. Beydoun, R. Amal, Mater. Sci. Eng. 94 (2002) 71–81.
[11] D. Beydoun, R. Amal, G. Low, S. McEvoy, J. Mol. Catal. A: Chem. 180 (2002) 193–200.
[12] S. Watson, J. Scott, D. Beydoun, R. Amal, J. Nanoparticle 7 (2005) 691–705.
[13] S. Xu, W. Shangguan, J. Yuan, M. Chen, J. Shi. Appl. Catal. B: Environ. 71 (2007) 177–184.
[14] S. Abramson, L. Srithammavanh, J.M. Siaugue, O. Horner, X. Xu, V. Cabuil, J. Nanoparticle 11 (2009) 459–465.
[15] Y. Gao, B. Chen, H. Li, Y. Ma, Mater. Chem. Phys. 80 (2003) 349–355.
[16] J. Xu, Y. Ao, D. Fu, C. Yuan, J. Phys. Chem. Solids 69 (2008) 1980–1984.
[17] T.A. Gad-Allah, S. Kato, S. Satokawa, T. Kojima, Desalination 244 (2009) 1–11.
[18] V. Belessi, D. Lambropoulou, I. Konstantiou, R. Zboril, J. Tucek, D. Jancik, T. Albanis, D. Petridis, Appl. Catal. B: Environ. 87 (2009) 181–189.
[19] R. Rosal, A. Rodriguez, J.A. Perdigon-Melon, A. Petre, E. Garcia-Calvo, M.J. Gomez, A. Aguera, A.R. Fernandez-Alba, Water Res. 44 (2010) 578–588.
[20] F. Méndez-Arriaga, S. Esplugas, J. Giménez, Water Res. 42 (2008) 585–594.
[21] I. Nicole, J. De Laat, M. Dore, J.P. Duget, C. Bonnel, Water Res. 24 (1990) 157–168.
[22] L. Yang, L.E. Yu, M.B. Ray, Environ. Sci. Technol. 43 (2009) 460–465.
[23] L. Yang, L.E. Yu, M.B. Ray, Water Res. 42 (2008) 3480–3488.
[24] N. Quici, M.E. Morgada, R.T. Gettar, M. Bolte, M.I. Litter, Appl. Catal. B: Environ. 71 (2007) 117–124.
[25] M.J. López-Muñoz, J. Aguado, B. Rupérez, Res. Chem. Interm. 33 (2007) 377–392.
[26] E.J. Rosenfeldt, K.G. Linden, Environ. Sci. Technol. 38 (2004) 5476–5483.
[27] F.J. Benítez, F.J. Real, J.L. Acero, G. Roldán, J. Chem. Technol. Biotechnol. 84 (2009) 1184–1195.
[28] X. Shi, N.S. Dalal, A.C. Jain, Food Chem. Toxicol. 29 (1991) 1–6.
[29] Y. Chen, C. Hu, X. Hu, J. Qu. Environ. Sci. Technol. 43 (2009) 2760–2765.